# Micro–Positron Emission Tomography Imaging of Cardiac Gene Expression in Rats Using Bicistronic Adenoviral Vector-Mediated Gene Delivery

Ian Y. Chen, MSE; Joseph C. Wu, MD; Jung-Jun Min, MD; Gobalakrishnan Sundaresan, PhD; Xiaoman Lewis, MD; Qianwa Liang, PhD; Harvey R. Herschman, PhD; Sanjiv S. Gambhir, MD, PhD

***Background***—We have previously validated the use of micro-positron emission tomography (microPET) for monitoring the expression of a single PET reporter gene in rat myocardium. We now report the use of a bicistronic adenoviral vector (Ad-CMV-D2R80a-IRES-HSV1-sr39tk) for linking the expression of 2 PET reporter genes, a mutant rat dopamine type 2 receptor (D2R80a) and a mutant herpes simplex virus type 1 thymidine kinase (HSV1-sr39tk), with the aid of an internal ribosomal entry site (IRES).

***Methods and Results***—Rat H9c2 cardiomyoblasts transduced with increasing titers of Ad-CMV-D2R80a-IRES-HSV1-sr39tk (0 to $2.5\times10^8$ pfu) were assayed 48 hours later for reporter protein activities, which were found to correlate well with viral titer ($r^2=0.96$, $P<0.001$ for D2R80A; $r^2=0.98$, $P<0.001$ for HSV1-sr39TK) and each other ($r^2=0.97$; $P<0.001$). Experimental (n=8) and control (n=6) athymic rats underwent intramyocardial injection of up to $2\times10^9$ pfu of Ad-CMV-D2R80a-IRES-HSV1-sr39tk and saline, respectively. Forty-eight hours later and weekly thereafter, rats were assessed for D2R80a-dependent myocardial accumulation of 3-(2-[$^{18}$F]fluoroethyl)spiperone ([$^{18}$F]-FESP) and HSV1-sr39tk–dependent sequestration of 9-(4-[$^{18}$F]fluoro-3-hydroxymethylbutyl)guanine ([$^{18}$F]-FHBG) using microPET. Longitudinal [$^{18}$F]-FESP and [$^{18}$F]-FHBG imaging of experimental rats revealed a good correlation between the cardiac expressions of the 2 PET reporter genes ($r^2=0.73$; $P<0.001$). The location of adenovirus-mediated transgene expression, as inferred from microPET images, was confirmed by ex vivo gamma counting of explanted heart.

***Conclusions***—The IRES-based bicistronic adenoviral vector can potentially be used in conjunction with PET for indirect imaging of therapeutic gene expression by replacing 1 of the 2 PET reporter genes with a therapeutic gene of choice. **(*Circulation*. 2004;109:1415-1420.)**

**Key Words:** gene therapy ■ imaging ■ nuclear medicine ■ myocardium



The majority of current clinical studies on cardiac gene therapy focus on evaluating the safety and efficacy of various therapeutic vectors and gene products.[1] There is, however, a lack of understanding on the kinetics and biodistribution of therapeutic gene expression in humans.[2] Preclinical studies on animal models have addressed these issues with the use of postmortem reporter gene assays,[3] but the invasiveness of these assays render them impractical for human applications. Recent advances in micro-positron emission tomography (microPET) technology have made possible noninvasive imaging of transgene expression in small living animals.[4] The results obtained from microPET studies can be directly confirmed in humans with existing clinical PET scanners. MicroPET findings on the kinetics and biodistribution of therapeutic gene expression should help to better evaluate the effectiveness of cardiac gene therapy in preclinical models.

MicroPET imaging of therapeutic gene expression and its pharmacokinetics can be theoretically achieved by either a direct or an indirect approach.[5] The direct approach involves imaging systemically delivered radioactive probes that can be preferentially accumulated by therapeutic gene products (eg, mRNA or enzyme) in cells containing the therapeutic gene. This approach, however, requires synthesizing a customized probe for every therapeutic gene of interest, thus lacking the generalizability that is needed for common gene therapy use. In contrast, the indirect approach makes use of a PET reporter gene whose expression can be feasibly imaged with a PET reporter probe. By coupling the expression of the PET reporter gene to that of a therapeutic gene, the therapeutic

Received July 11, 2003; de novo received October 2, 2003; accepted November 25, 2003.

From the Crump Institute for Molecular Imaging (I.Y.C., J.C.W., J.M., G.S., X.L., H.R.H., S.S.G.), Biomedical Physics Interdepartmental Graduate Program (I.Y.C.), Department of Molecular and Medical Pharmacology (J.C.W., J.M., G.S., X.L., H.R.H., S.S.G.), Department of Biochemistry/Molecular Biology Institute (Q.L., H.R.H.), and Department of Medicine, Division of Cardiology (J.C.W.), UCLA School of Medicine, Los Angeles, Calif.

Correspondence to Sanjiv S. Gambhir, MD, PhD, Stanford University, The James H. Clark Center, 318 Campus Dr, East Wing, First Floor, Stanford, CA 94305-5427. E-mail sgambhir@stanford.edu



***Circulation*** **is available at http://www.circulationaha.org** **DOI: 10.1161/01.CIR.0000121727.59564.5B**

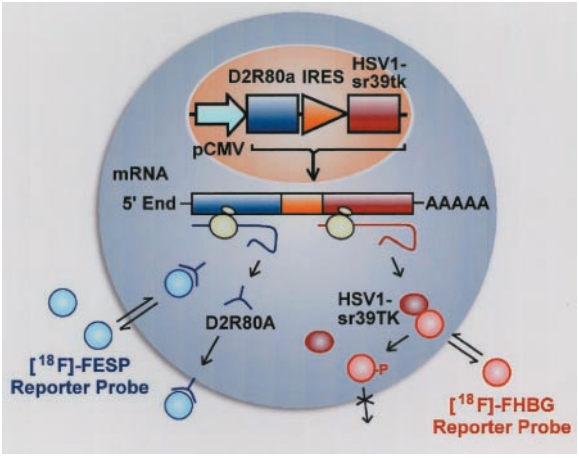


**Figure 1.** Schematic of Ad-CMV-D2R80a-IRES-HSV1-sr39tk–mediated gene expression. A CMV promoter drives expression of a single mRNA containing D2R80a and HSV1-sr39tk cistrons, separated by an EMCV IRES. Upstream cistron (D2R80a) and downstream cistron (HSV1-sr39tk) are translated by ribosome binding to 5′cap and IRES, respectively. Translated product of D2R80a (D2R80A) binds to [$^{18}$F]-FESP mainly on cell membrane, whereas translated product of HSV1-sr39tk (HSV1-sr39TK) phosphorylates [$^{18}$F]-FHBG and traps it intracellularly.

gene expression can be inferred indirectly from the PET reporter gene expression. This approach is preferred because the same PET reporter gene can be used with every therapeutic gene of interest as long as a strong correlation persists between the expression of therapeutic and PET reporter genes.

Two PET reporter genes, herpes simplex virus type 1 thymidine kinase (HSV1-tk)[4] and rat dopamine type 2 receptor (D2R),[6] have been developed and validated for use in indirect imaging of therapeutic gene expression. Their mutants, HSV1-sr39tk[7] and D2R80a,[8] have also been created by site-directed mutagenesis for enhanced imaging sensitivity and minimization of physiological side effects. Various approaches to coupling the expression of a PET reporter gene to that of a therapeutic gene are being actively investigated.[9] These include a fusion approach, internal ribosomal entry site (IRES) approach, double promoter approach, covector administration approach, and bidirectional transcriptional approach. In this study, we aimed to focus on the IRES approach and explore its use for indirect myocardial imaging.

We recently validated the use of microPET for detecting the expression of a single PET reporter gene, HSV1-sr39tk, in rat myocardium, using 9-(4-[$^{18}$F]fluoro-3-hydroxymethylbutyl)guanine ([$^{18}$F]-FHBG) as PET reporter probe.[10] Our goal in this study was to examine the use of an IRES-based bicistronic adenoviral vector (Ad-CMV-D2R80a-IRES-HSV1-sr39tk) for coupling the expression of 2 PET reporter genes (Figure 1). The vector we specifically constructed contains a cytomegalovirus (CMV) early promoter driving the expression of 2 PET reporter genes, a mutant rat D2R (D2R80a) and a mutant HSV1-tk (HSV1-sr39tk), with the aid of an encephalomyocarditis virus (EMCV) IRES. Here, we show using microPET that the bicistronic adenoviral vector, when injected into the myocardium of living rats, leads to correlated myocardial expression of the 2 PET reporter genes. With further refinement of this vector by replacing one of the PET reporter genes with a therapeutic gene of interest (eg, vascular endothelial growth factor, VEGF), the IRES-based strategy should allow for indirect imaging of therapeutic gene expression by imaging PET reporter gene expression.

## Methods

### Construction, Purification, and Characterization of Recombinant Adenovirus

A replication-defective adenovirus (Ad-CMV-D2R80a-IRES-HSV1-sr39tk) carrying a CMV early promoter driving the expression of 2 PET reporter genes, a mutant herpes simplex virus type 1 thymidine kinase (HSV1-sr39tk, 1.1 kb) and a mutant rat dopamine type 2 receptor (D2R80a, 1.3 kb), with the aid of an EMCV IRES was constructed, purified, and characterized as previously described.[8] The reporter proteins corresponding to D2R80a and HSV1-sr39tk are referred to here as D2R80A and HSV1-sr39TK, respectively.

### In Vitro Assays for HSV1-sr39TK and D2R80A Activities in Rat H9c2 Cardiomyoblasts

H9c2 cardiomyoblasts (American Type Culture Collection) were cultured as previously described[11] and transduced with varied viral titers of Ad-CMV-D2R80a-IRES-HSV1-sr39tk. Forty-eight hours later, cell lysates were assayed for both D2R80A binding and HSV1-sr39TK enzyme activity using [$^{3}$H]spiperone binding[6] and [$^{3}$H]penciclovir phosphorylation assays.[7] H9c2 cells transduced with equal titers of Ad-CMV-fluc (an adenovirus carrying CMV early promoter driving firefly luciferase [fluc]) were used as negative controls.

### Myocardial Injection of Adenovirus

Eight athymic nu/nu rats (200 to 300 g; Charles River Laboratories, Wilmington, Mass) and 8 immunocompetent Sprague-Dawley rats (200 to 300 g; Charles River Laboratories, Wilmington, Mass) underwent aseptic survival surgery according to protocols approved by the UCLA Animal Research Committee. Rats received isoflurane for general anesthesia (2%), banamine (2.5 mg/kg) for pain relief, atropine (40 $\mu$g/kg) for prevention of bradycardia, and normal saline (4 mL) for volume replacement. Rats were anesthetized, intubated, and mechanically ventilated before undergoing left thoracotomy for access to the left ventricle. Replication-defective adenovirus diluted in 40 $\mu$L of PBS was injected directly at one site into the anterolateral wall at a rate of $\approx$8 $\mu$L per second. After that, air was expelled from the chest, and the chest wounds were sutured closed. Six additional athymic nu/nu rats were similarly injected with 40 $\mu$L of saline and served as negative controls.

### MicroPET Imaging of Cardiac Reporter Gene Expression

MicroPET imaging of cardiac reporter gene expression was performed with a dedicated small-animal microPET scanner.[12] After induction and maintenance of anesthesia with 5% and 2% isoflurane, rats were injected by tail vein with [$^{13}$N]ammonia (2.57$\pm$0.12 mCi) and imaged for 20 minutes to verify perfusion and to locate the position of the heart in the scanner field of view. After that, rats were injected with either 3-(2-[$^{18}$F]fluoroethyl)spiperone ([$^{18}$F]-FESP; 2.78$\pm$0.42 mCi) or [$^{18}$F]-FHBG (2.78$\pm$0.40 mCi), rested for either 3 hours ([$^{18}$F]-FESP) or 1 hour ([$^{18}$F]-FHBG) to allow for tracer uptake and clearance, and then imaged for 15 minutes over the chest, covering the heart and the lungs. Raw images were reconstructed using filtered backprojection, and the pixel counts were decay-corrected to scan start time.

### Quantitative PET Data Analysis

MicroPET images were acquired as a set of fifteen 1.2-mm transaxial slices covering the entire 18-mm axial scanner field of view. Slices

showing distinct myocardial accumulation of [$^{18}$F]-FHBG or [$^{18}$F]-FESP were averaged by use of a customized software CRIIISP to form a new image, from which a region of interest (ROI) of 2.92-mm radius was drawn. The average count rate (counts/second per pixel) within the ROI was determined and converted to tracer activity (mCi/mL) using a calibration constant obtained by microPET scanning of a 35-mm-diameter cylindrical phantom filled with known $^{18}$F activity concentration. Assuming a tissue density of 1 g/mL, tracer activity (mCi/g) was then divided by the injected dose (mCi) to obtain a tissue uptake index in percent injected dose per gram of tissue (% ID/g). Another ROI was obtained similarly from the contralateral lung field 3.6 mm superior to the myocardial ROI, and its tissue uptake (%ID/g) was determined similarly. The ratio of heart to lung tissue uptakes was then calculated and is referred to here as the normalized [$^{18}$F]-FESP or [$^{18}$F]-FHBG activity.

### Gamma Counting of $^{18}$F Radioactivity in Explanted Heart

After microPET scans, explanted hearts were counted for $^{18}$F radioactivity in a gamma well counter (Cobra II Auto-Gamma, Packard) as previously described.[10]

### Statistical Analysis

Linear regression analysis was performed to assess the linear relationship between 2 variables. The strength of correlation between them was quantified in terms of the square of Pearson product-moment correlation coefficient ($r^2$). The significance of correlation was obtained by performing Student's $t$ test against the null hypothesis that the correlation coefficient ($r$) is zero. A probability value $<0.05$ was considered statistically significant.

## Results

### In Vitro Assays on Rat H9c2 Cardiomyoblasts Revealed Correlated HSV1-sr39TK and D2R80A Activities

To assess how well the IRES-based bicistronic adenoviral vector (Ad-CMV-D2R80a-IRES-HSV1-sr39tk) leads to expression of 2 PET reporter genes (D2R80a and HSV1-sr39tk) in cell culture, we transduced rat H9c2 cardiomyoblasts with increasing titers of adenovirus (0, $0.5\times10^8$, $1\times10^8$, $1.5\times10^8$, $2\times10^8$, and $2.5\times10^8$ pfu) and assayed them 48 hours later for both HSV1-sr39TK and D2R80A activities. Over the range of viral titer used, both D2R80A binding and HSV1-sr39TK enzyme activity increase linearly with increasing viral titer and correlate well with viral titer (Figure 2A, $r^2=0.96$, $P<0.001$ for D2R80A; Figure 2B, $r^2=0.98$, $P<0.001$ for HSV1-sr39TK). Neither protein activity exhibits saturation at the highest viral titer used. A strong correlation ($r^2=0.97$; $P<0.001$) also exists between the activities of the 2 PET reporters (Figure 2C).

### MicroPET Imaging Revealed Correlated [$^{18}$F]-FESP and [$^{18}$F]-FHBG Accumulations in Both Athymic and Immunocompetent Rats

To assess the transgene expression of D2R80a and HSV1-sr39tk after intramyocardial gene delivery, we used microPET to quantitatively image the D2R80a-dependent accumulation of [$^{18}$F]-FESP and HSV1-sr39tk–dependent sequestration of [$^{18}$F]-FHBG. We performed weekly [$^{18}$F]-FESP and [$^{18}$F]-FHBG scans for as long as 4 months on 8 athymic rats intramyocardially injected with various titers of Ad-CMV-D2R80a-IRES-HSV1-sr39tk ($1\times10^7$ to $2\times10^9$ pfu). The [$^{18}$F]-FESP and [$^{18}$F]-FHBG scans were done on

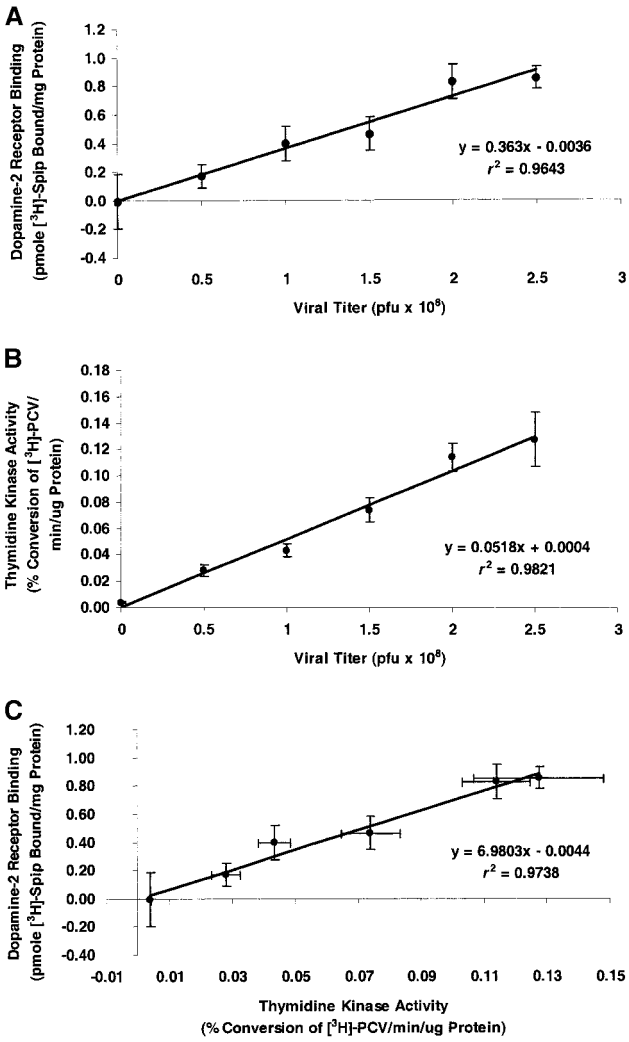


**Figure 2.** In vitro HSV1-sr39TK enzyme activity and D2R80A binding. Rat H9c2 cardiomyoblasts were transduced with increasing viral titers (0, $0.5\times10^8$, $1\times10^8$, $1.5\times10^8$, $2\times10^8$, $2.5\times10^8$ pfu) of Ad-CMV-D2R80a-IRES-HSV1-sr39tk. Forty-eight hours later, cell lysates were assayed for (A) D2R80A binding and (B) HSV1-sr39TK enzyme activity. (C) D2R80A binding is plotted against HSV1-sr39TK enzyme activity for each viral titer. Error bars represent SEM of triplicates.

consecutive days, irrespective of order, so that the expression of HSV1-sr39tk and D2R80a could be compared as close in time as possible. Figure 3, A and B, shows representative transaxial [$^{18}$F]-FESP and [$^{18}$F]-FHBG images acquired, overlaid with an [$^{13}$N]ammonia myocardial perfusion scan. Distinct myocardial [$^{18}$F]-FESP and [$^{18}$F]-FHBG accumulations are seen in the anterolateral wall, confirming the successful delivery and expression of both D2R80a and HSV1-sr39tk. Figure 3, C and D, shows the typical coronal [$^{18}$F]-FESP and [$^{18}$F]-FHBG images of the thorax. The lung activity is notably higher in the [$^{18}$F]-FESP than in the [$^{18}$F]-FHBG image. Although the [$^{18}$F]-FESP tissue uptakes (%ID/g) pooled from all scans and from all rats correlate poorly ($r^2=0.42$; $P<0.001$) with the [$^{18}$F]-FHBG tissue uptakes, the normalized [$^{18}$F]-FESP activities correlate well ($r^2=0.73$; $P<0.001$) with the normalized [$^{18}$F]-FHBG activities (Figure 4). For the 6 control rats, which received saline alone, the normalized

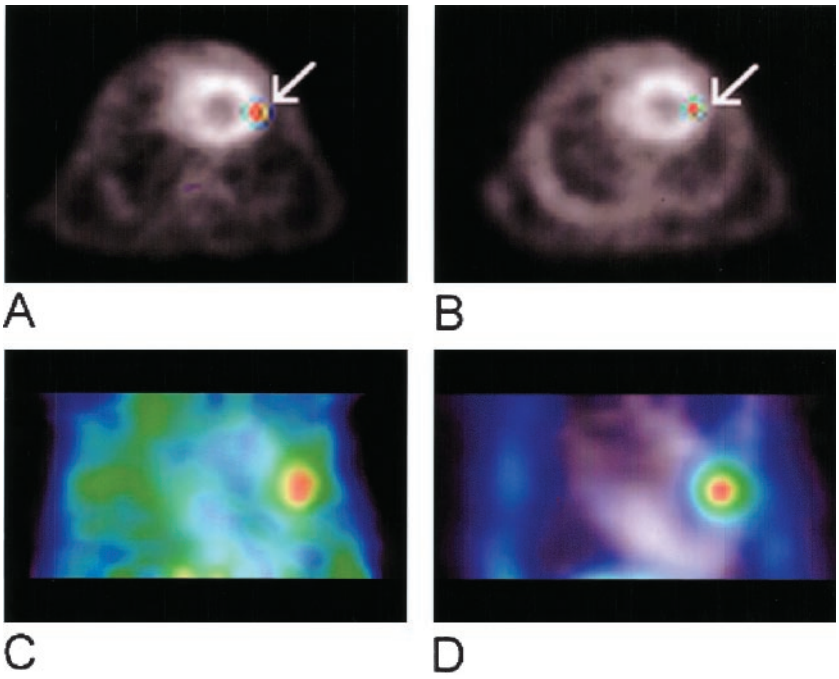


**Figure 3.** [18F]-FESP and [18F]-FHBG accumulations in rat myocardium. An athymic rat was injected intramyocardially with $2\times10^9$ pfu of Ad-CMV-D2R80a-IRES-HSV1-sr39tk and scanned (A) on day 2 for D2R80a-dependent accumulation of [18F]-FESP and (B) on day 3 for HSV1-sr39tk–dependent sequestration of [18F]-FHBG. Transaxial [18F]-FESP and [18F]-FHBG images (color) are individually superimposed on an [13N]ammonia perfusion scan (gray scale) for easier localization of tracer accumulation relative to myocardium. Distinct tracer accumulation (arrow) is seen in anterolateral wall of myocardium, corresponding to site of viral injection. Coronal (C) [18F]-FESP and (D) [18F]-FHBG images of thorax, individually overlaid with an [13N]-ammonia perfusion scan, show that lung activity is notably higher in [18F]-FESP than in [18F]-FHBG image, probably because of a slower clearance of [18F]-FESP from lung parenchyma.

[18F]-FESP and [18F]-FHBG activities on days 2 and 3 are $0.849\pm0.09$ and $1.097\pm0.186$, respectively. As expected, viral titer correlates poorly with either [18F]-FESP or [18F]-FHBG accumulation (data not shown), most likely as a result of variable viral trafficking after intramyocardial delivery. The lowest viral titer detected on microPET images is $1\times10^7$ pfu. To assess whether correlated D2R80a and HSV1-sr39tk expressions can also be observed in the presence of immune response, we performed biweekly [18F]-FESP and [18F]-FHBG scans on 8 immunocompetent rats injected intramyocardially with $1\times10^9$ pfu of Ad-CMV-D2R80a-IRES-HSV1-sr39tk. Collectively, the normalized [18F]-FESP activities correlate well with the normalized [18F]-FHBG activities ($r^2=0.76$; $P<0.001$; data not shown); the correlation is worse when the myocardial uptakes (%ID/g) between [18F]-FESP and [18F]-FHBG are compared ($r^2=0.06$; $P<0.5$).

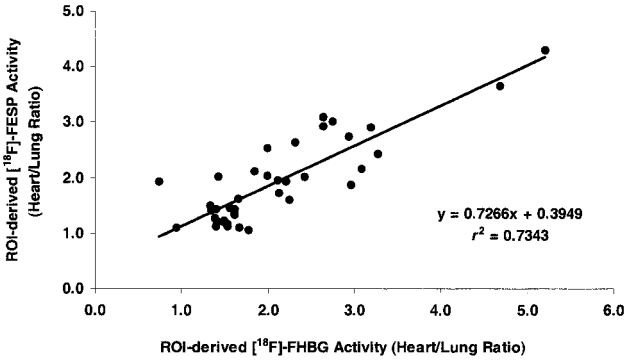


**Figure 4.** Correlation between ROI-derived myocardial [18F]-FESP and [18F]-FHBG activities. Eight athymic rats injected with up to $2\times10^9$ pfu of Ad-CMV-D2R80a-IRES-HSV1-sr39tk were imaged longitudinally for D2R80a-dependent myocardial accumulation of [18F]-FESP and HSV1-sr39tk–dependent accumulation of [18F]-FHBG. Weekly [18F]-FESP activities (eg, days 2, 9, 16, etc) for all rats are plotted against corresponding weekly [18F]-FHBG activities (eg, days 3, 10, 17, etc). Data are not shown for weeks in which either [18F]-FESP or [18F]-FHBG was not available for microPET scanning. ROI-derived myocardial activity is normalized by ROI-derived lung activity, and ratio is expressed as a unitless index.

## Ex Vivo 18F Gamma Counting of Explanted Heart Confirmed the Source of Myocardial Activity Observed on MicroPET Images

Eleven rats injected with varied titers of Ad-CMV-D2R80a-IRES-HSV1-sr39tk ($1\times10^7$ to $2\times10^9$ pfu) were killed after either a positive [18F]-FESP (n=6) or a positive [18F]-FHBG scan (n=5), and their hearts were explanted for ex vivo gamma counting. Both ROI-derived [18F]-FESP and [18F]-FHBG activities correlate well with ex vivo gamma activity after [18F]-FESP and [18F]-FHBG scans, respectively (Figure 5A, $r^2=0.86$, $P<0.01$ for [18F]-FESP; Figure 5B, $r^2=0.83$, $P<0.05$ for [18F]-FHBG).

## Discussion

We have validated the use of an IRES-based bicistronic adenoviral vector (Ad-CMV-D2R80a-IRES-HSV1-sr39tk) for coupling the myocardial expression of 2 PET reporter genes (D2R80a and HSV1-sr39tk) after intramyocardial gene delivery. Using in vitro reporter protein assays and microPET imaging of living rats, we found a good correlation between the PET reporter activities not only in rat H9c2 cardiomyoblasts ($r^2=0.97$; $P<0.001$) but also in the myocardium of living athymic rats ($r^2=0.73$; $P<0.001$). Although the in vivo correlation is slightly weaker, probably because of case-by-case variation in tracer delivery and transport kinetics that is circumvented in cell culture, for general use in cardiac gene therapy, this level of correlation should allow one to reliably infer the expression of the therapeutic gene from that of a linked PET reporter gene, which can be imaged quantitatively with PET.

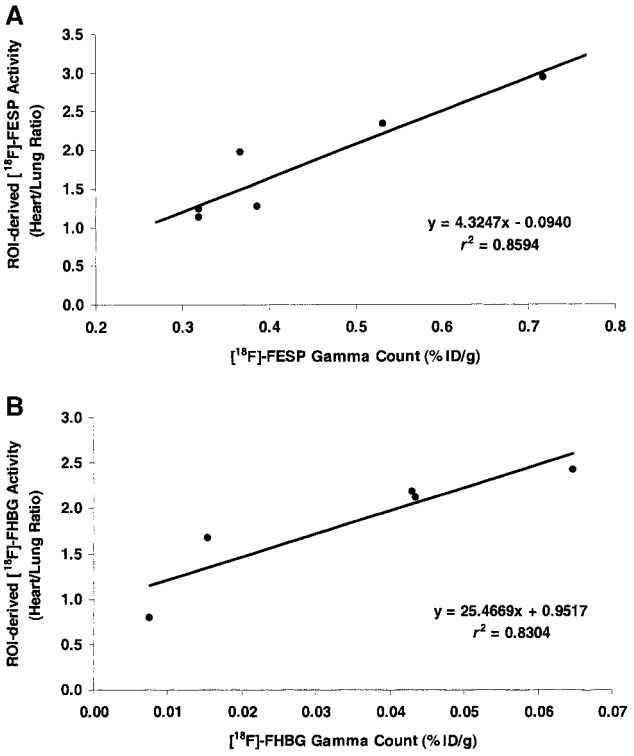


**Figure 5.** Ex vivo gamma counting of explanted heart. In 11 rats, heart was explanted after either a positive (A) [$^{18}$F]-FESP or (B) [$^{18}$F]-FHBG scan and counted for $^{18}$F gamma activity in a well counter. For each tracer, gamma activity is plotted against its ROI-derived myocardial activity normalized by ROI-derived lung activity.

In this study, we used 2 PET reporter gene/reporter probe systems: HSV1-sr39tk/[$^{18}$F]-FHBG and D2R80a/[$^{18}$F]-FESP. The former has been specifically validated for cardiac applications[10]; we now report the first use of the latter system specifically for myocardial imaging. Compared with HSV1-sr39tk, D2R80a has the advantage of being endogenous and therefore should elicit minimal immune response and lead to prolonged adenovirus-mediated transgene expression in rat myocardium.[13] The [$^{18}$F]-FESP reporter probe, however, has been found to lead to a higher lung activity than [$^{18}$F]-FHBG in this study, presumably because of a slower tissue clearance from sites without D2R80a expression. On some [$^{18}$F]-FESP images, the elevated lung activity appears to spill over into the myocardial ROI, causing a slight decrease in contrast (Figure 3C). This spillover, however, is not limiting because the gamma counting of explanted heart correlates well with the ROI-derived [$^{18}$F]-FESP activity ($r^2$=0.86; $P$<0.01). Quantitatively, the elevated lung activity is reflected in the lower normalized activity for [$^{18}$F]-FESP than [$^{18}$F]-FHBG and consequently the slope of the in vivo [$^{18}$F]-FESP and [$^{18}$F]-FHBG correlation curve being <1 (Figure 4). A slope of 0.73 favoring the normalized [$^{18}$F]-FHBG activity implies that for the range of viral titer used in this study, the overall cardiac signal-to-background ratio for the D2R80a/[$^{18}$F]-FESP system is ≈30% less than that of the HSV1-sr39tk/[$^{18}$F]-FHBG system. On the basis of signal generation alone, the HSV1-sr39tk/[$^{18}$F]-FHBG system is advantageous over the D2R80a/[$^{18}$F]-FESP system.

In analyzing microPET data, we tried 2 indices for quantifying cardiac tracer tissue uptake: %ID/g and the ratio of ROI-derived heart to lung activities. The former is a crude measure of tissue uptake that relies on an assumed injected dose. It is sensitive to errors associated with tail vein injection, which may result from either extravasation or adherence of "sticky" tracer (eg, [$^{18}$F]-FESP) to the syringe, leading to as much as 8% to 10% residual activity. In contrast, the latter index is designed to partially correct for problems associated with injection or tracer, assuming that both heart and lung activities reflect the amount of tracer that actually entered the circulation. The ratio approach was found in this study to yield a much higher in vivo correlation ($r^2$=0.73; $P$<0.001) between the myocardial [$^{18}$F]-FESP and [$^{18}$F]-FHBG accumulations in athymic rats compared with the case when %ID/g was used ($r^2$=0.42; $P$<0.001). Extensions of this approach involving tracer kinetic modeling and input function determination according to methods previously developed in our laboratory[14] will be necessary to improve quantification further.

In addition to PET quantification, immune response to either viral antigens or reporter gene products presents another major challenge to longitudinal imaging of therapeutic and reporter gene expressions. We have previously succeeded in monitoring adenovirus-mediated reporter gene expression in immunocompetent rats for ≈2 weeks, but not much longer because of the mounting of an intense host immune response.[10] To examine the behavior of Ad-CMV-D2R80a-IRES-HSV1-sr39tk for a much longer period, we used athymic rats in this study to minimize immune response while simulating the case clinically when the subject is immunosuppressed. We then repeated experiments in immunocompetent rats to investigate whether host immune response would alter IRES-mediated translation or specifically the coupling between the expressions of HSV1-sr39tk and D2R80a. Using microPET, we demonstrated that Ad-CMV-D2R80a-IRES-HSV1-sr39tk leads to correlated reporter gene expression not only in athymic ($r^2$=0.73; $P$<0.001) but also immunocompetent ($r^2$=0.76; $P$<0.001) rats, supporting the notion that IRES-mediated translation is stable in the presence of immune response. The bicistronic gene expression, however, could be imaged for only ≈2 to 3 weeks, and in one rare exception 2 months, in immunocompetent rats, compared with at least 4 months in athymic rats. Hence, future applications of the bicistronic construct should involve the use of less immunogenic viruses (eg, "gutless" adenovirus) for gene delivery to prolong transgene expression.[15] It will be important in the long run that the PET reporter gene also does not elicit a significant immune response. For human applications, the D2R80a PET reporter gene may have to be changed from the rat sequence to the human sequence, and HSV1-sr39tk may need to be used in conjunction with immunosuppressive medications. These extensions of the current work, although straightforward, will require further validation.

A major drawback associated with any IRES-based bicistronic vector is that the downstream transgene expression is often attenuated.[16] For future application of the bicistronic vector, it will be ideal to place the therapeutic gene upstream of IRES if maximal therapeutic effect is desired or the

reporter gene upstream if utmost imaging sensitivity is needed. Alternatively, a "super-IRES" element can be engineered from short segments of cellular mRNA and cloned into the bicistronic vector to enhance downstream transgene expression by as much as 63-fold over the EMCV IRES element.[17] Should D2R80a be used as a PET reporter gene for myocardial imaging of living rats, methods to correct for lung spillover, injection error, and residual activity in the needle should be implemented to improve PET quantification. If HSV1-sr39tk is desired, then means to minimize immune response should be undertaken to prolong transgene expression. Depending on whether D2R80a or HSV1-sr39tk is used, there would be a size limit of 3.8 or 4.0 kb to the therapeutic gene with our present adenoviral vector backbone. This size constraint, however, can be relaxed to ≈30 kb by using high-capacity "gutless" adenovirus.[15] Last, cardiac specific promoter (eg, cardiac myosin light chain 2), which can minimize hepatic expression after intramyocardial gene delivery, should be used in place of the constitutive CMV promoter to prevent potential side effects arising from injection-related viral leakage to the circulation.[10] Ultimately, with further refinement of the vector and improvement in PET quantification, the IRES-based bicistronic vector design should enable noninvasive imaging of the kinetics and biodistribution of therapeutic gene expression (eg, VEGF) in not only rat but also human myocardium.

## Acknowledgments

This work was supported in part by NIH grants R0-1-CA-82214 (Dr Gambhir), SAIRP R24-CA-92865 (Dr Gambhir), Department of Energy Contract DE-FC03-87ER60615 (Dr Gambhir), and AHA Western Affiliate Postdoctoral Grant (Dr Wu). We thank Judy Edwards and Waldemar Ladno for assisting with microPET image acquisition and reconstruction.

## References

1. Isner JM. Myocardial gene therapy. *Nature*. 2002;415:234–239.
2. Pislaru S, Janssens SP, Gersh BJ, et al. Defining gene transfer before expecting gene therapy: putting the horse before the cart. *Circulation*. 2002;106:631–636.
3. Huard J, Lochmuller H, Acsadi G, et al. The route of administration is a major determinant of the transduction efficiency of rat tissues by adenoviral recombinants. *Gene Ther*. 1995;2:107–115.
4. Gambhir SS, Barrio JR, Phelps ME, et al. Imaging adenoviral-directed reporter gene expression in living animals with positron emission tomography. *Proc Natl Acad Sci U S A*. 1999;96:2333–2338.
5. MacLaren DC, Toyokuni T, Cherry SR, et al. PET imaging of transgene expression. *Biol Psychiatry*. 2000;48:337–348.
6. MacLaren DC, Gambhir SS, Satyamurthy N, et al. Repetitive, noninvasive imaging of the dopamine D2 receptor as a reporter gene in living animals. *Gene Ther*. 1999;6:785–791.
7. Gambhir SS, Bauer E, Black ME, et al. A mutant herpes simplex virus type 1 thymidine kinase reporter gene shows improved sensitivity for imaging reporter gene expression with positron emission tomography. *Proc Natl Acad Sci U S A*. 2000;97:2785–2790.
8. Liang Q, Satyamurthy N, Barrio JR, et al. Noninvasive, quantitative imaging in living animals of a mutant dopamine D2 receptor reporter gene in which ligand binding is uncoupled from signal transduction. *Gene Ther*. 2001;8:1490–1498.
9. Ray P, Bauer E, Iyer M, et al. Monitoring gene therapy with reporter gene imaging. *Semin Nucl Med*. 2001;31:312–320.
10. Wu JC, Inubushi M, Sundaresan G, et al. Positron emission tomography imaging of cardiac reporter gene expression in living rats. *Circulation*. 2002;106:180–183.
11. Bengel FM, Anton M, Avril N, et al. Uptake of radiolabeled 2′-fluoro-2′-deoxy-5-iodo-1-β-D-arabinofuranosyluracil in cardiac cells after adenoviral transfer of the herpesvirus thymidine kinase gene: the cellular basis for cardiac gene imaging. *Circulation*. 2000;102:948–950.
12. Cherry SR, Gambhir SS. Use of positron emission tomography in animal research. *ILAR J*. 2001;42:219–232.
13. Quinones MJ, Leor J, Kloner RA, et al. Avoidance of immune response prolongs expression of genes delivered to the adult rat myocardium by replication-defective adenovirus. *Circulation*. 1996;94:1394–1401.
14. Green LA, Gambhir SS, Srinivasan A, et al. Noninvasive methods for quantitating blood time-activity curves from mouse PET images obtained with fluorine-18-fluorodeoxyglucose. *J Nucl Med*. 1998;39:729–734.
15. Kochanek S, Schiedner G, Volpers C. High-capacity "gutless" adenoviral vectors. *Curr Opin Mol Ther*. 2001;3:454–463.
16. Yu Y, Annala AJ, Barrio JR, et al. Quantification of target gene expression by imaging reporter gene expression in living animals. *Nat Med*. 2000;6:933–937.
17. Chappell SA, Edelman GM, Mauro VP. A 9-nt segment of a cellular mRNA can function as an internal ribosome entry site (IRES) and when present in linked multiple copies greatly enhances IRES activity. *Proc Natl Acad Sci U S A*. 2000;97:1536–1541.

# Micro–Positron Emission Tomography Imaging of Cardiac Gene Expression in Rats Using Bicistronic Adenoviral Vector-Mediated Gene Delivery

Ian Y. Chen, Joseph C. Wu, Jung-Jun Min, Gobalakrishnan Sundaresan, Xiaoman Lewis, Qianwa Liang, Harvey R. Herschman and Sanjiv S. Gambhir

*Circulation.* 2004;109:1415-1420; originally published online March 8, 2004;
doi: 10.1161/01.CIR.0000121727.59564.5B
*Circulation* is published by the American Heart Association, 7272 Greenville Avenue, Dallas, TX 75231

Print ISSN: 0009-7322. Online ISSN: 1524-4539